Journal of Coastal Research	SI	51	87-94	West Palm Beach, Florida	Summer 2010

Tidally-averaged Currents and Bedload Transport over the Kwinte Bank, Southern North Sea

Erwan Garel [1*]

[1] School of Ocean and Earth Science
National Oceanography Centre
Southampton (NOCS),
European Way
Southampton, SO14 3ZH
United Kingdom

[*] Present address: CIACOMAR
University of Algarve
Avenida 16 de Junho
8700-311 Olhão
Portugal
egarel@ualg.pt

ABSTRACT

The short-term dynamics of a dredged tidal sandbank (the Kwinte Bank, southern North Sea) are examined, on the basis of field measurements and 1D sediment transport modelling. The field measurements include current data from shipborne Acoustic Doppler Current Profiler (ADCP) and from moorings (ADCP and electromagnetic S4), collected across the bank during a nominal (spring) tidal cycle, and during 7 tidal cycles, respectively. The dynamics of the bank are described in terms of tidally-averaged (residual) currents and (net) bedload transport.

The results indicate a predominance of ebb flow during the period of study. Convergence of (net) bedload transport is predicted, from both flanks towards the crest of the bank. The exact location of the sand transport convergence zone varies, in the short-term, according to the prevailing tidal currents. The observation of clockwise veering of the peak ebb and flood currents over the bank indicates that this sediment transport pattern relates, at least partially, to tidal rectification of the flow.

In relation to dredging, the present study suggests that the presence of a (dredged) depression at the crest of the bank influences locally the short-term hydrodynamics. The currents are channelised, and the across-bank peak (near-bed) flow is enhanced towards the crest. Net erosion of the depression is predicted, over the tidal cycle considered. More data are needed to evaluate the morphological evolution of the trough over the long-term.

ADDITIONAL INDEX WORDS: *sandbank, short-term dynamics, dredging.*

INTRODUCTION

Sandbanks are present on continental shelves, in shelf seas and within estuarine environments. They occur in areas characterised by strong currents, capable of moving the sand, and an abundance of sand, supplied from the local seabed or coastal erosion (DYER and HUNTLEY, 1999). Although many studies have attempted to describe their morphodynamic behaviour (for reviews, see DYER and HUNTLEY, 1999; PATTIARATCHI and COLLINS, 1987; and WRIGHT, 1995), there is no overall consensus on the processes of sandbank formation and maintenance. Several classifications have been proposed, to account for their diverse morphology, regional setting, formation and development (e.g. DYER and HUNTLEY, 1999; and PATTIARATCHI and COLLINS, 1987).

This study concerns tidal sandbanks which are defined as open shelf linear ridges (Type I, according to the classification of DYER and HUNTLEY, 1999). Typically, these sand bodies present an asymmetric cross-section profile, with a main axis oriented at an angle to the peak tidal flow. These features are 13 km wide, on average, tens of metres in height, and up to 80 km in length. Amongst a number of theories to explain the existence of this type of sandbank, the "seabed stability analysis" approach (HUTHNANCE, 1982a, b), is the most promising. The model considers water and sand movements as an interacting system, which is described on the basis of coupled hydrodynamic and sediment dynamic equations. The theory relates the existence of tidal sandbanks to the deflection of flow over the bank (tidal rectification). Such deflection is explained by increasing bottom friction (over the seafloor elevation), resulting in a deceleration of the along-bank component of the flow, together with acceleration of the across-bank component, in order to satisfy continuity. As such, the currents veer as they move on to the bank, resulting in sediment transport towards the crest. On the downstream side of the bank, the current is weaker, due to friction over the bank. Thus, sediment transport takes place mainly on the upstream side, towards the top of the deposit. Consequently, for reversing tidal flow, net convergence of sand occurs over the crest. In addition, the Coriolis force generates vorticity, due to compression of the water column over the bank. This effect tends to enhance the deflection and, hence, the growth of the banks which are aligned cyclonically (anti-clockwise, in the northern hemisphere), relative to the flow (STRIDE, 1982; and ZIMMERMAN, 1981). The morphology (orientation and wavelength) of numerous tidal sandbanks supports the above concept, at least, qualitatively (BELDERSON, JOHNSON, and KENYON, 1982; CASTON, 1972;

DOI: 10.2112 / SI51-008.1 received 15 January 2007; accepted in revision 24 September 2007.

KENYON *et al.*, 1981; LANCKNEUS and DE MOOR, 1995, and PATTIARATCHI and COLLINS, 1987).

This contribution focuses upon the short-term hydro-sediment dynamics over the Kwinte Bank, a tidal sandbank in the southern North Sea (Figure 1.). Intense sand extraction (see below) has created depressions at the crest of the bank. Although of importance to a number of environmental issues (e.g. coastal erosion) and to a sustainable management of the resource, the morphodynamic response of the bank to dredging is largely unknown. In this study, both hull-mounted and moored current-meters are used to examine the tidally-averaged currents over the bank. Residual bedload sediment transport patterns are derived using a one-dimensional (1D) sediment transport model. The aims are to examine maintenance processes associated with the bank, together with the near-field hydro-sediment dynamic impact of dredging.

ENVIRONMENTAL SETTING

The Kwinte Bank is part of the Flemish sandbank system (Figure 1.), a group of Quaternary sand bodies deposited on Tertiary (Ypresian) units (mainly clays) (BERNÉ *et al.*, 1994; LE BOT *et al.*, 2005). These banks are considered to be in, or close to, an equilibrium state, maintained by the present-day flow conditions (STRIDE, 1982). The Kwinte Bank is about 15 km in length, 10-20 m in height, and 1 to 2 km in width (i.e. about 400 Mm^3 in volume). The minimum water depth lies close to 5 m MLLWS (Mean Lowest Low-Water at Spring), over its southern part. The bank is aligned in a NE-SW direction. It shows a strongly asymmetric profile, being steeper towards the NW. The area experiences semi-diurnal progressive tides, macrotidal in range (4-5 m). The average tidal ellipse is elongated along a NE-SW axis, rotated some degrees clockwise from the Kwinte Bank orientation. The tidal currents rotate counter-clockwise, with maximum currents (about 1 m/s) observed generally during the flood, towards the NE (CASTON, 1972; DE MOOR, 1986; HOUBOLT, 1968; and VAN CAUWENBERGHE, 1971). Small to large 3D compound dunes (ASHLEY, 1990) cover extensively the bank (LANCKNEUS and DE MOOR, 1991) (e.g. Figure 2.). On the basis of the direct observation of the asymmetry of small dunes on side-scan sonar imagery, LANCKNEUS *et al.* (1992) consider that the flood and ebb are dominant on the western and eastern part of the bank, respectively, inducing sand transport, from the adjacent swales, towards the crest. Such convergence of sand transport, over a tidal cycle, is considered to play a major role in the build up of the bank. The exact location and extension of the areas over which residual sand transport is either dominated by the peak flood or ebb currents, appears to vary significantly, over time (LANCKNEUS *et al.*, 1992). Vertical growth of the bank is limited probably by wave and storm action, i.e. the stirred sediments are redistributed over the flanks, where they reintegrate into the maintenance mechanism.

Intense sand extraction has taken place from the Kwinte Bank, since 1979, by trailer suction dredging (DEGRENDELE *et al.*, this volume). This activity has formed two particular depressions, located along the crestline, in the northern and central parts of the bank. The central depression is the area excavated the most, with dimensions of about 700 m in width, 1 km in length and up to 5 m in depth (Figure 2.). Dredging at this location ceased in February 2003, for a 3 year period, to allow monitoring of the evolution (and potential recovery) of the sand extraction zone. To date, no regeneration of the depression has been identified, on the basis of sequential swath bathymetric surveys (DEGRENDELE *et al.*, this volume).

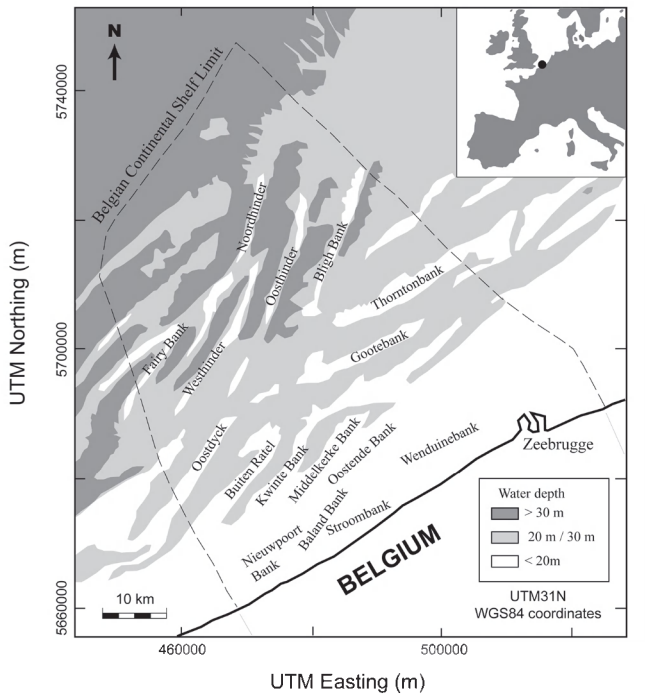

Figure 1. Location map of the sandbanks on the Belgian Continental Shelf (modified from Deleu et al., 2004). Note: bathymetric contours relative to the Mean Lowest Low-Water at Spring (MLLWS).

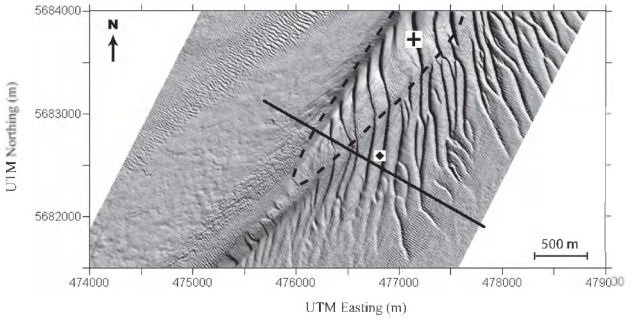

Figure 2. Shaded relief map of the central part of the Kwinte Bank (illuminated from the southwest), based upon swath bathymetry (grid data from the Marine Sand Fund for Extraction). Key: black line-location of the repeated hull-mounted ADCP profiles; diamond- S4 deployment site; cross- bottom-mounted ADCP location; and the dashed line indicates the limits of the central dredged depression (see text).

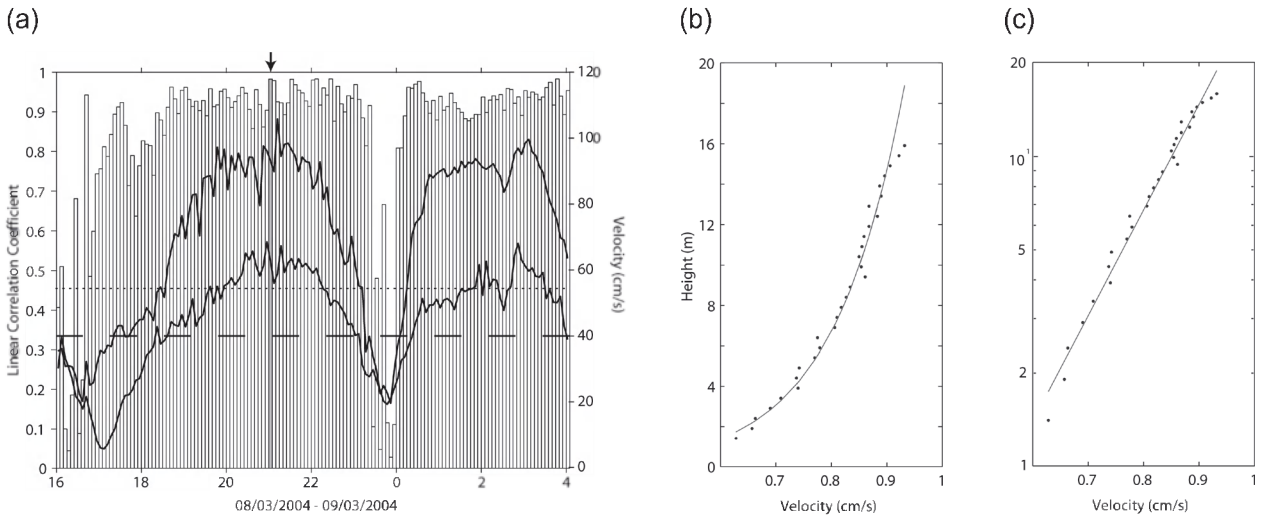

Figure 3. (a) Linear correlation coefficient for the logarithmic velocity distribution throughout the water column (bars), together with the near-surface and near-bed current velocities from the BM-ADCP (solid lines, the near-surface currents being generally faster). Key: dashed line- approximate threshold for significant sand transport by tidal currents; dotted line- critical correlation coefficient, at a 99 % confidence level; the arrow and the grey bar indicate the example shown in (b) and (c). (b) Velocity profile observed at 21h. on 8th March 2004 (measurements (dots) and line of best fit); and (c), as (b), plotted on a logarithmic depth scale.

METHODS

Data Acquisition

Flow velocities were recorded, over the Kwinte Bank, using 3 instruments (Figure 2.): (1) a moored 1200 kHz (RDI) Acoustic Doppler Current Profiler (ADCP), operating at 0.3 Hz, from 1.4 m up to 16.4 m above the seafloor, with a resolution of 0.5 m (hereafter BM-ADCP, for Bottom-Mounted ADCP); (2) a S4 electromagnetic current meter (Model ADW, INTEROCEAN) operating at 2 Hz, at 0.75 m from the seabed (hereafter S4); (3) a 300 kHz ADCP (RDI), mounted in the hull of the R/V *Belgica* (hereafter HM-ADCP, for Hull-Mounted ADCP), operating at 1 Hz, at 1 m intervals, from 7 m below the water surface (due to the vessel draught and the blanking period), to 2-3 m above the sea bed. The latter rejects errors due to contamination of the signal with the reflection from the seabed. Herein, '*near-bed currents*' refers to the ADCP bin lying closest to the sea bottom, and to the S4 records; likewise, '*near-surface currents*' to the ADCP bin closest to the water surface.

The moorings were deployed between the 2nd and 11th March 2004, at the northern extremity of the central dredged depression (BM-ADCP) and at the crest of the bank (S4), at 9 and 11 m MLLWS, respectively (Figure 2.). The present contribution focuses upon measurements undertaken under mild meteorological conditions, between the 7th and 10th March (with W-SW wind < 8 m/s, and insignificant wave action near the sea bed). HM-ADCP data were collected on the 8th and 9th March, during a (nominal) 13 hour cycle on spring tides. Fifteen tracks were repeated along a profile being perpendicular to the bank axis (including the dredged depression), at around 3 knots (1.5 m/s) (Figure 2.). The navigation data were acquired with a Differentially-corrected Geographical Positioning System (DGPS), precise to within $^{+}$1 m.

Data Processing

BM-ADCP records were averaged every 100 pings inside the data acquisition system, to reduce measurement uncertainties; this provided an averaged current velocity and direction, every 8 min and 20 s. The HM-ADCP transmitted averaged data to an onboard PC, every 30 pings; these data were processed and averaged to a horizontal sampling interval of 180 m (i.e. 10 averaged values along the profile). The S4 was set up to provide averaged current fluctuations over 9 min, every 15 min.

Sediment transport was computed using the 1D sediment transport model SEDTRANS05 (Neumeier *et al.*, in press), an improved version of SEDTRANS96 (for details, see Li and Amos, 2001). Bottom shear stresses have been derived from the averaged near-bed currents, using the Grant and Madsen (1986) bottom boundary layer approach. Bedload sediment transport, using the skin-friction shear stress, has been computed based upon the algorithm for non-cohesive material of Yalin (1963), for currents alone. The Yalin equation applies to a grain-size of 0.2 mm, or coarser. For a grain-size of 0.45 mm, Gadd, Lavelle, and Swift, (1978) consider that the algorithm yields predictions of transport rates which are in relatively good agreement with flume data, at velocities near the threshold of movement. Sediment transport simulations were carried out using the distribution of the mean grain-size (d50) over the study area, established on the basis of recent sediment sampling campaigns (Bellec *et al.*, this volume). The mean grain size was 0.3 and 0.8 mm at the S4 and BM-ADCP locations, respectively; it ranged from 0.25 to 0.4 mm along the HM-ADCP tracks. The bedform dimension inputs into the model (wavelength = 2.5 m; height = 0.35 m) were derived from side-scan sonar imagery acquired during the survey (Garel, Manso, and Collins, 2005).

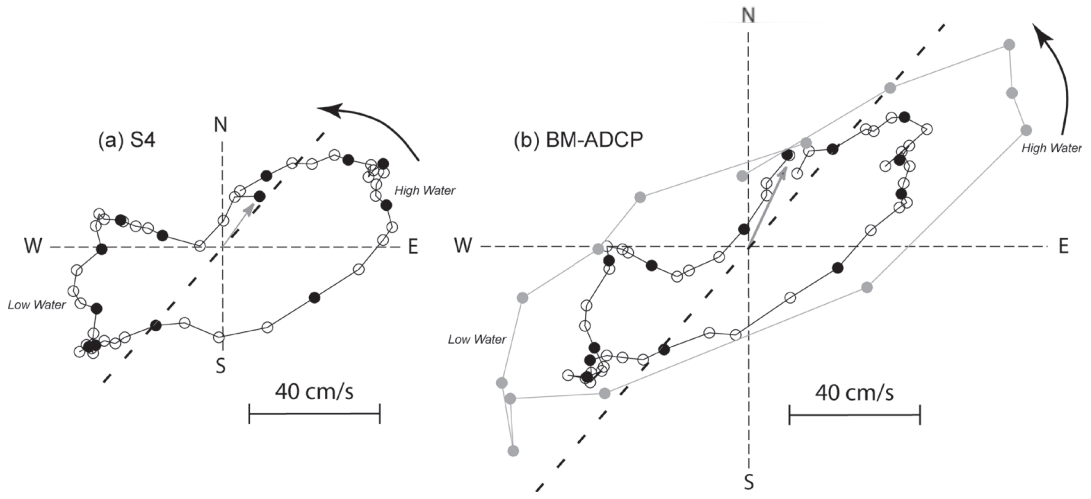

Figure 4. Typical tidal ellipse, as recorded by the S4 (a) and BM-ADCP ((b): black- near-bed currents; grey- near-surface currents). The selected tidal cycle is that shown in Figure 3a. Key: the grey vector denotes currents at the beginning of the experiment; small circles represent 15 min time-steps, for the current vectors (1 hour-time step for the circles filled with black). Arrows outside the ellipse denote the direction of the vector rotation. The dashed line indicates the bank axis.

For the sediment transport calculations, the model considers the velocity profile to be logarithmic within the turbulent boundary layer. This assumption was tested over a single tidal cycle, based upon the BM-ADCP measurements. The correlation coefficient (r) for the 'goodness-of-fit' to a logarithmic profile is shown in Figure 3. The trend exists, at a confidence level of 99 %, if r is above a critical value of 0.463 (DAVIS, 2002). The fit of the measurements to the logarithmic profile is very good, with r generally about 0.9 (Figure 3a.). Examples of an observed velocity profile are presented in Figures 3b. and 3c. Poor correlation is observed only around the slack waters, when the bed sediment is not mobile (for example, SOULSBY (1997) considers that significant sand transport takes place for tidal current in excess of about 40 cm/s). Therefore, the velocity profiles can reasonably be considered as logarithmic, for the sediment transport calculations.

Inherent to the method of data acquisition, the sampling time interval of the HM-ADCP data was not regular at fixed locations along the profile. Thus, in this case, the tidally-averaged currents and sediment transport were obtained by applying a trapezoidal rule. Concerning the Eulerian measurements (i.e. BM-ADCP and S4), the tidally-averaged values correspond to the mean, over the tidal cycle which was considered.

RESULTS

Bottom-mounted instruments

An example of the records from the moored current meters, during the same tidal cycle as Figure 3., is presented in Figure 4. The tidal ellipses display the regional tidal features, i.e. a dominantly (anti-clockwise) progressive tidal wave, with SW-NE trending peak currents rotated 15-25° (clockwise) to the axis of the bank. These observations are consistent with previous data sets available for the area, on the basis of *in-situ* measurements (such as free drifting buoy experiments) and numerical modelling outputs (VAN LANCKER *et al.*, 2004; and WILLIAMS *et al.*, 2000). In detail, the main axis of the tidal ellipse lies closer to the orientation of the depression at the BM-ADCP location, than at the crest (S4). This observation persists over the (4 day) period of the records. In the selected example (Figure 4.), peak flood currents (towards the NE) are similar in magnitude to the peak on the ebb, with faster currents observed with greater distance from the bed. However, at both locations, the peak currents last longer during the ebb, than the flood. For example, the near-bed currents are > 40 cm/s during approximately 3h45min of the ebb and 3h of the flood (see Figure 3.). Such a difference is important in terms of the tidally-averaged (net) sediment transport. The tidal currents over the 4 day period show high variability in the peak currents patterns, over time and with location (Figure 5a.). Ebb asymmetry is not observed for all the tides, e.g. Tide 7 in Figure 5a., where the flood is prevailing. Furthermore, for any given tide, the ebb or the flood may predominate, depending upon location on the bank (e.g. Tides 2 or 3, where the tidal asymmetry is apparent for one instrument, only). Consequently, the residual current vectors show distinct orientation, depending of the tidal cycle and instrument considered (Figure 5b.). At the crest (S4), the residual currents are constantly towards the southwest. In contrast, the residual currents from the BM-ADCP data are directed either towards the northeast, or the west. Residual current magnitudes are similar at both locations, of up to 8 cm/s (Figure 5c.).

Due to the non-linearity of sediment transport, in response to the prevailing flow conditions, net sand transport patterns do not correspond necessarily to the directions of the residual currents. The net bedload transport directions are either flood- or ebb- dominated, depending upon the tidal cycle considered (Figure 5d.). Tides 6 and 7 are ebb and flood dominated, re-

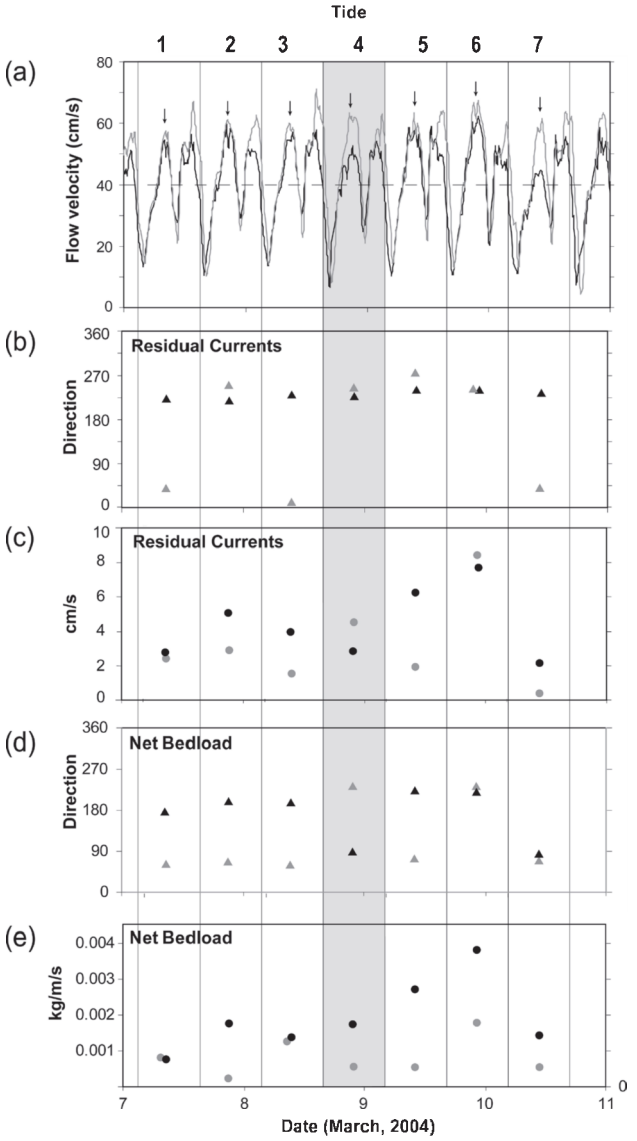

Figure 5. Comparison of the flow, residual currents and net sediment transport, from the S4 (black) and BM-ADCP (grey) data (the vertical grey area indicates the particular tidal cycle corresponding to Figures 3a, 4, and to the HM-ADCP data): (a) near-bed current magnitude (arrows indicate the peak ebb currents); (b) residual near-bed current direction; (c) residual near-bed current magnitude; (d) net bedload transport direction; (e) net bedload transport magnitude.

spectively. In other cases, the model indicates opposing net sand transport directions at crest and at the depression, i.e. sand convergence between these two sites. Bedload transport rates are slightly greater at crest, with values up to ~0.004 kg/m/s (Figure 5e.).

Hull-mounted ADCP

The residual currents computed from the shipborne ADCP data, over a single tidal cycle (Tide 4, Figure 5.), are consistent with those obtained from the moorings (Figures 5b., 5c. and 6.). The vectors are orientated (mainly) towards the west-southwest. Thus, ebb flows predominate over the study area, during this tidal cycle. In detail, the near-surface and near-bed residuals present similar directions and magnitude over the crest (Figure 6.). Probably, the reduced water depth at this location induces a more uniform behaviour of the currents along the water column than elsewhere across the bank. The near-surface residual current directions are deviated progressively clockwise, towards the western flank of the bank; this is associated with a decrease in magnitude (from 20 cm/s, in the East, to 10 cm/s, in the West). In contrast, the near-bed currents are deflected (clockwise) only over the upper lee slope and crest, associated with the strongest residuals (up to 14 cm/s).

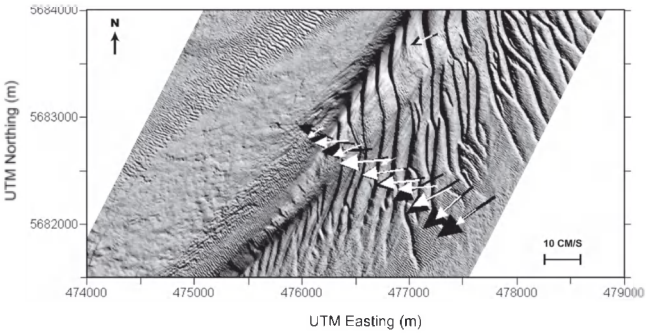

Figure 6. Residual near-bed (white arrows) and near-surface (black arrows) currents, based upon the HM-ADCP data.

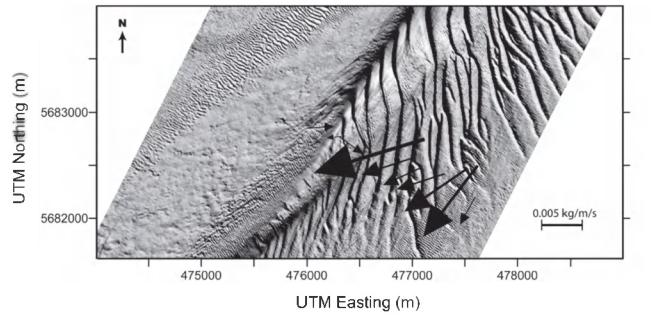

Figure 7. Net bedload transport across the bank, based upon the HM-ADCP data.

The net bedload transport predictions are shown in Figure 7. Overall, transport is towards the SW, i.e. the general direction of the residual currents (Figure 6.). In detail, the potential net transport lies sub-parallel to the bathymetric contour at the foot of the eastern flank and veers progressively 45° clockwise, towards the crest of the bank. In contrast, the transport is towards the E-NE over the western flank. Further, divergent transport pathways are predicted inside the depression. The highest transport rates (up to 0.014 kg/m/s) are at the crest and over the eastern flank of the bank, which compare with the residual currents.

DISCUSSION

Hydrodynamic numerical modelling of the tidal flow, over the Kwinte Bank area, was integrated over an 11 day period (Brière *et al.*, this volume) and over a complete spring-neap tidal cycle (14.8 days) (Van Lancker *et al.*, 2004; Van den Eynde *et al.*, this volume). These models describe anti-clockwise gyres, centred over the adjacent swales, whose position or scale varies with the tidal flow conditions. The near-bed tidally-averaged flow magnitudes and directions described here are in good agreement with the outputs of these models, averaged over several tidal cycles (e.g. Brière *et al.*, this volume). Thus, the records of the present study are considered to be typical of tidal flow conditions over the bank, i.e. rather than being generated by exceptional (non-tidal) conditions. Ebb predominance over the bank appears to be more important than was considered previously.

Repeated seafloor mapping surveys undertaken over the Kwinte Bank, during 4 years, indicate a slow and constant propagation rate (of up to 10 m/yr) for the large dunes, towards the NE (Degrendele *et al.*, this volume); this is in agreement with their asymmetry (Bellec *et al.,* this volume). However, net sand transport directions towards the SW are (often) proposed in the present study (Figure 7.; Figure 5d.). These striking differences relate to the time-scale of the observations. From side-scan sonar data, Garel, Manso, and Collins. (2005) reported elsewhere the complete reversal of small dunes, on the western rim of the depression, during a single tidal cycle. In contrast, the asymmetry of the larger bedforms is indicative of net sediment transport over a longer time scale (Berné *et al.*, 1993; Lanckneus and de Moor, 1995). In this case, the bedform dynamics is governed by the dominant tidal flow and, probably, (shorter term) storm events. For example, based upon numerical modelling, Van den Eynde *et al.* (this volume) consider that the influence of waves over the Kwinte Bank may alter drastically the direction of the residual sediment transport.

In the short-term, the present data indicate prevailing ebb and flood sand transport pathways, on each flank of the bank, respectively; as such, sand convergence up to the crest (Figure 7.; Figure 5d.). This pattern is consistent with the modelling results of Brière, Roos, and Garel. (this volume) and Van den Eynde *et al.* (this volume). Previously, Lanckneus *et al.* (1992), and, more recently, Bellec *et al.* (this volume), arrived at the same interpretation, based upon bedform asymmetries. Lanckneus *et al.* (1992) consider that areas in which the net sand transport direction is controlled, either by the flood or the ebb phase of the tide, varies significantly with time. Such variations are consistent with fluctuations in the net transport directions, observed at the mooring sites, over various tidal cycles (Figure 5d.).

The stability model proposed by Huthnance (1982a, b) depicts sand convergence up to a bank crest, in response to tidal rectification of the flow. At the Kwinte Bank, the angle observed (sometimes) between the crest of the large and (superimposed) small bedforms, suggests veering in the sand transport pathways, towards the crest (e.g. Figure 6. in Bellec *et al.*, this volume). However, as noted by Dyer and Huntley (1999), acceleration and refraction of tidal flows over sandbanks have proved to be difficult to identify in the field. Difficulties arise from the highly localised nature of the flow refraction. Good examples of tidal rectification originate from Ocean Surface Current Radar measurements over the Middelkerke Bank, which lies adjacent to the Kwinte Bank (Figure 1.) (Williams *et al.*, 2000), and from shipborne ADCP measurements obtained across the Shambles Bank, in the English Channel (Bastos, Paphitis, and Collins, 2004). Following the approach of Bastos, Paphitis, and Collins. (2004), HM-ADCP data were used to identify deflection of the flow over the bank. Peak ebb and flood current velocities throughout the water column were transformed into perpendicular along-bank (positive towards the NE) and across-bank (positive towards the NW) components, and displayed in a 50 m horizontal- and 1 m vertical-resolution grid (Figure 8.). Acceleration of the across-bank component, together with retardation of the along-bank component over the bank, can be observed along some of the tracks. This flow pattern is consistent with tidal rectification over the bank, providing a mechanism for the convergence of sand towards the crest. Thus, a part of the maintenance processes of the bank can be described successfully by the sea bed stability model.

The (dredged) depression has been found to affect the short-term near-field hydro-sediment dynamics. The distinct orientation of the main axis of the tidal ellipses, over the depression (BM-ADCP) and at the crest (S4), suggests a channelisation of the peak (tidal) currents over the depression (Figure 4.). The veering of the crest of the very large dunes, inside the depression, is indicative of a persistent pattern, predominantly in the flood direction, in the long-term. Bellec *et al.* (this volume) support this interpretation, based upon morphological and sedimentological considerations. However, the differences in the observed tidal ellipses might relate to site effects, e.g. the position of the instrument with respect to the very large dunes; additional measurements, including moored current-meters together with swath bathymetry, are required to investigate this point. Besides, near-bed peak currents show, on occasions, specific flow patterns inside the depression; these are restricted to the depression, suggesting a local effect, as proposed by Degrendele *et al.* (this volume). For example, the across-bank component of the flood flow within the depression (Figure 8a.), is stronger near the bed than in the overlying cells. Moreover, the across-bank components of the peak ebb flow, inside and above the depression are in opposite directions (Figure 8c.). In both examples, the near-bed across-bank flow is enhanced towards the crest, in the trough. In this way, localised sediment transport may be significantly affected. Such flow patterns are not observed systematically in the records. Their significance in terms of net sediment transport and morphological evolution of the depression should be considered on the basis of a data set with a higher vertical resolution (i.e. < 1 m). Nonetheless, divergent net sand transport directions are predicted inside the depression (Figure 7.), indicating net erosion, over the tidal cycle studied. Since the depression has not recovered since extraction ceased (Degrendele *et al.*, this volume), erosion induced by divergent net sand transport may be a persistent active process, inside the depression.

CONCLUSIONS

The processes which govern sandbank dynamics in the long-term are difficult to identify, on the basis of short-term hydrodynamic measurements. In the present study, tidally-averaged currents and residual sediment transport patterns are computed, for the Kwinte Bank, by using moored and

shipborne current meter data. The results contribute to understanding the maintenance processes of the bank, and the near-field hydro-sediment dynamic impact of sand extraction, at this particular location.

The tidally-induced, short-term, sand transport pattern over the Kwinte Bank is characterised by sand convergence towards the crest of the bank. The location of the convergence zone varies, in the short-term, according to the prevailing tidal flow characteristics. Sediment transport over each flank of the bank is governed by a distinct phase of the tide. During peak flood and ebb flows, tidal rectification, in response to enhanced bed friction, provides a mechanism for the veering of sand towards the crest of the bank. As such, the sea bed stability model described by HUTHNANCE (1982a, b) accounts, at least partially, for the bank maintenance process.

The presence of the dredged depression affects, on a local basis, the short-term hydrodynamics and sediment transport patterns. The collected data support the concept of channelisation of peak tidal flows, at this particular location. In addition, within the depression, the cross-bank components of the peak near-bed currents are enhanced towards the crest of the bank. Divergent net sand transport is induced within the trough. Hence, the depression experienced net erosion over the tidal cycle considered. More data are needed to detail the structure of the flow within the trough, and to investigate the morphodynamic evolution of this feature over the long-term.

ACKNOWLEDGEMENTS

This study was undertaken as part of the EUMARSAND Research Training Network (European Sand and Gravel Resources: Evaluation and Environmental Impact of Extraction, HPRN-CT-2002-00222). The assistance of the officers and crew of the research vessel R/V *Belgica*, in collecting the data, is gratefully acknowledged. Thanks are extended to Dries Van den Eynde, for providing the meteorological data and to the Management Unit of the North Sea Mathematical Models (MUMM), for assistance during the field campaign and the use of the hull-mounted and bottom-mounted ADCP data. The University of Dunkerque is acknowledged for the deployment of the S4 current meter. Professor Michael Collins (NOCS, Southampton, U.K, and AZTI-Technalia, Spain) is thanked for his comments on early draft of the manuscript.

LITERATURE CITED

ASHLEY, G.M., 1990. Classification of large-scale subaqueous bedforms: a new look at an old problem, *Journal of Sedimentary Petrology*, 60(1), 60-172.

BASTOS, A.C.; PAPHITIS, D., and COLLINS, M.B., 2004. Short-term dynamics and maintenance processes of headland-associated sandbanks: Shambles Bank, English Channel, UK, *Estuarine Coastal and Shelf Science,* 59, 33-47.

BELDERSON, R.H.; JOHNSON, M.A., and KENYON, N.H., 1982. Bedforms. *In*: STRIDE, A.H. (ed.), *Offshore Tidal Sands: Processes and Deposits*. London: Chapman & Hall, 27-57.

BELLEC, V.; VAN LANCKER, V.; DEGRENDELE, K.; ROCHE, M., and LE BOT, S., this volume. Geo-environmental characterization of the Kwinte Bank. *Journal of Coastal Research*.

BERNÉ, S.; CASTAING, P.; LE DREZEN, E., and LERICOLAS, G., 1993. Morphology, internal structure and reversal of asymmetry of large subtidal dunes in the entrance to Gironde Estuary (France), *Journal of Sedimentary Research,* 65(5), 780-793.

BERNÉ, S.; TRENTESAUX, A.; STOLK, A.; MISSIAEN, T., and DE BAPTIST, M., 1994. Architecture and long-term evolution of a tidal sand-bank: the Middelkerke Bank (southern North Sea). *Marine Geology*, 121, 57-72.

BRIÈRE, C.; ROOS, P., and GAREL E., this volume. Modeling the morphodynamic effects of sand extraction on the Kwinte Bank. *Journal of Coastal Research*.

CASTON, V.N.D., 1972. Linear sand banks in the southern North Sea. *Sedimentology*, 18, 63-78.

DAVIS, J.C., 2002. *Statistics and data analysis in Geology, 3rd Edition*. New York: John Wiley & Sons, 646 p.

DELEU, S.; VAN LANCKER, V.; VAN DEN EYNDE, D., and MOERKERKE, G., 2004. Morphodynamic evolution of the kink of an offshore tidal sandbank: the Westhinder Bank (Southern North Sea). *Continental Shelf Research*, 24, 1587-1610.

DEGRENDELE, K.; ROCHE, M.; SCHOTTE, P.; VAN LANCKER, V.; BELLEC, V., and BONNE, W., this volume. Morphological evolution of the Kwinte Bank central depression before and after cessation of aggregate extraction. *Journal of Coastal Research*.

DE MOOR, G., 1986. Geomorfologisch onderzoek op het Belgisch Continental Plat. *Tijdschrift van de Belg. Ver. Aarddr. Studies BEVAS 2*, 133-174.

DYER, K.R. and HUNTLEY, D.A., 1999. The origin, classification and modeling of sand banks and ridges. *Continental Shelf Research*, 19, 1285-1330.

GADD, P.E.; LAVELLE, J.W., and SWIFT, D.J.P., 1978. Estimates of sand transport on the New York shelf using near-bottom current-meter observations. *Jour. Sed. Pet.*, 48(1), 239-252.

GAREL, E.; MANSO, F., and COLLINS, M.B., 2005. Hydrodynamics and sediment transport during a tidal cycle on the Kwinte Bank (Southern North Sea), *Proceedings of the 5th Conference of Coastal Dynamics* (Barcelona, Spain, ASCE), 135-136.

GRANT, W.D. and MADSEN, O.S., 1986. The continental shelf bottom boundary layer. *Ann. Rev. Fluid Mech.*, 18, 265-305.

HOUBOLT, J.J.H.C., 1968. Recent sediments in the Southern Bight of the North Sea. *Geologie & Mijnbouw*, 47(4), 245-273.

HUTHNANCE, J.M., 1982a. On one mechanism forming linear sandbanks, *Estuarine, Coastal and Shelf Science*, 14, 79-99.

HUTHNANCE, J.M., 1982b. On the formation of sandbanks of finite extent, *Estuarine, Coastal and Shelf Science*, 15, 277-299.

KENYON, N.H.; BELDERSON, R.H.; STRIDE, A.H., and JOHNSON, M.A., 1981. Offshore tidal sandbanks as indicator of net sand transport and as potential deposits. *In*: *Holocene Marine Sedimentation in the North Sea Basin 5*, (ed. Nio, S.D., Shuttenhelm, R.T.E., Van Weering, TC.E.), Blackwell Science, 257-268.

LANCKNEUS, J. and DE MOOR, G., 1991. Present-day day evolution of sandwaves on a sandy shelf bank in the southern Bigh, *Oceanologica Acta*, Vol. Sp. 11, 123-127.

LANCKNEUS, J.; DE MOOR, G.; DE SCHAEPMEESTER, G., and DE WINNE, E., 1992. Monitoring of a tidal sandbank: Evolution of bedforms, volumetric trends, sedimentological changes. *Hydro '92, Eight Biennial International Symposium of the Hydrographic Society* (Copenhagen, Denmark), 19 p.

LANCKNEUS, J. and DE MOOR, G., 1995. Bedforms on the Middelkerke bank, southern North Sea, *In*: *Tidal Signatures in Modern and Ancient Sediments* (ed. Flemming, B.W., Bartholoma, A.), Blackwell Science, 35-51.

LE BOT, S.; VAN LANCKER, V.; DELEU S.; DE BATIST, M.; HENRIET J.P., and HAEGEMAN, W., 2005. Geological and geotechnical properties of

Eocene and Quaternary deposits on the Belgian continental shelf: a synthesis. *Netherlands Journal of Geosciences*, 84(2), 147-160.

Li, M. Z. and Amos, C. L., 2001. SEDTRANS96: the upgraded and better calibrated sediment-transport model for continental shelves, *Computers & Geosciences*, 27, 619-645.

Neumeier, U.; Ferrarin, C.; Amos, C.L.; Umgiesser, G., and Li, M.Z. (in press). Sedtrans05: An improved sediment-transport model for continental shelf and coastal waters, including a new algorithm for cohesive sediments, *Computer & Geosciences*.

Pattiaratchi, C.B. and Collins, M.B., 1987. Mechanisms for linear sandbank formation and maintenance in relation to dynamical oceanographic observations. *Progress in Oceanography*, 19, 117-176.

Soulsby, R L., 1997. Dynamics of Marine Sands. London : Thomas Telford Publications, 249 p.

Stride, A.H., 1982. Offshore Tidal Sands. Process and Deposition. London: Chapman & Hall, 222 p.

Van Cauwenberghe, C., 1971. Hydrografische analyse van de Vlaamse banken langs de Belgische-Frans kust. *Ingenieurdtijdingen Blatt*, 20, 141-149.

Van den Eynde, D.; Giardino, A.; Portilla, J.; Fettweis, M.; Francken, F., and Monbaliu, J., this volume. Modelling the effects of sand extraction on the sediment transport due to tides on the Kwinte Bank. *Journal of Coastal Research*.

Van Lancker, V.; Deleu, S.; Bellec, V.; Le Bot, S.; Verfaillie, E.; Fettweis, M.; Van Den Eynde, D.; Francken, F.; Pison, V.; WartelL, S.; Monballiu, J.; Portilla, J.; Lanckneus, J.; Moerkerke, G., and Degraer, S., 2004. Management, research and budgeting of aggregates in shelf seas related to end-users (Marebasse), *Scientific Report Year 2*, Belgian Science Policy, 144 p.

Williams, J.J.; MacDonald, N.J.; O'Connor, B.A., and Pan, S., 2000. Offshore sand bank dynamics, *Journal of Marine Systems,* 24, 153-173.

Wright, L.D., 1995. Morphodynamics of Inner-Continental shelves. Boca Raton: Marine Science Series, CRC Press, 233 p.

Yalin, M.S., 1963. An expression for bedload transportation. *Jour. Hydraul. Div. Proc.* ASCE, 89, HY3, 221-250.

Zimmerman, J.T.F., 1981. Dynamics, diffusion and geomorphological significance of tidal residual eddies. *Nature*, 290, 549-555.